LA-UR -87-2804

CONF 870973--14

Los Alamos National Laboratory is operated by the University of California for the United States Department of Energy under contract W-7405-ENG-36

LA-UR--87-2804

DE87 014767

TITLE NUCLEATION AND GROWTH OF $^3$He-B IN $^3$He-A

AUTHOR(S) G. W. Swift, P-10

SUBMITTED TO LT-18, Kyoto, Japan
August 20-26, 1987

## DISCLAIMER



Los Alamos

Los Alamos National Laboratory
Los Alamos, New Mexico 87545

FORM NO 836 R4
ST NO 2629 5/81

MASTER

DISTRIBUTION OF THIS DOCUMENT IS UNLIMITED

# Nucleation and Growth of $^3$He-B in $^3$He-A

C. W. SWIFT AND D. S. BUCHANAN*

(Condensed Matter and Thermal Physics Group, Los Alamos National Laboratory, Los Alamos, New Mexico 87545 USA)

The $^3$He A → B transition is remarkable for a number of reasons. Because of the small bulk free energy difference between the two phases, the probability of homogeneous thermal nucleation of the B phase is vanishingly small. Thus the experimental fact that the B phase nucleates readily from the A phase is not understood. The A → B transition is also remarkable in that when it occurs after cooling from above the critical temperature, it occurs in an extreme state of supercooling known as hypercooling. In this situation, the velocity of propagation of the A-B phase interface is controlled by microscopic phenomena rather than by thermal diffusion. We briefly review our recent work on both these topics, including the velocity of propagation of the A-B interface through hypercooled $^3$He-A, a search for cosmic-ray-induced B-phase nucleation, and preliminary observations of B-phase nucleation locations and temperatures.

## 1. INTRODUCTION: THE STATIONARY A-B INTERFACE

Of all the first-order phase transitions that occur in nature, the $^3$He A → B transition is among the most remarkable. The $^3$He A-B interface provides us with a boundary between two macroscopic quantum states having different symmetries. The stationary A-B interfacial surface tension is a consequence of the spatially smooth transition between the A- and B-phase order parameters that takes place at this boundary. This surface tension was originally measured by Osheroff and Cross [1] and interpreted by them [2] and by Kaul and Kleinert [3]; more recently, Schopohl [4] has calculated the surface tension more accurately. Other recent work on the stationary A-B interface includes Yip's [5] theoretical studies of the Kapitza resistance of the A-B interface and of Onsager-like relations coupling heat flow through the interface with the pressure difference across the interface, and Salomaa's [6] theoretical study of the topology of exotic vortices terminating on a rotating A-B interface.

## 2. THE MOVING A-B INTERFACE

The A → B transition is also remarkable in that it exhibits extremely large supercooling. When the A → B transition takes place after cooling from above the superfluid transition temperature, it occurs at a very low reduced temperature $T_n/T_{AB}$, where $T_n$ is a nucleation temperature, $T_{AB}$ is the equilibrium, thermodynamic transition temperature, and both are functions of pressure. At commonly observed values of $T_n$ the adiabatic temperature rise for the A → B phase transition, $L/C$, where $L$ is the latent heat of the transition per unit volume and $C$ is the specific heat per unit volume, is much less than the temperature difference $T - T_n$. Indeed at melting pressure $L/C$ is about 10 μK while we have observed values of $T_{AB} - T_n$ in excess of 400 μK. Such a material is said to have been hypercooled: supercooled so far below the equilibrium transition temperature, with nucleation at $T_n$, that $C(T_{AB}-T_n)/L > 1$. While hypercooling has been observed in other materials [7], the A → B transition in $^3$He is also remarkable in that far greater degrees of hypercooling can be observed in it than in any other substance.

For ordinary supercooling, where $C(T_{AB}- T_n)/L < 1$, the velocity of propagation of the interface between two phases is determined by straightforward thermal considerations [8], involving the diffusion of the latent heat of the transition away from the interface. But for a hypercooled transition the latent heat can be absorbed locally by the heat capacity, so that some other mechanism must limit the velocity of propagation. We have measured the velocity of A-B interface propagation through hypercooled $^3$He-A to be as large as 67 cm/s. For the case of an A → B transition in supercooled $^3$He a preliminary calculation [9] estimated the thermally limited velocity of propagation to be ca. 0.05 cm/s.

For measurements of the velocity of propagation $v_{AB}$, our experimental cell was a heavy-walled epoxy vessel with a c... ...l open column for $^3$He, shown in Fig. 1a, enclosed in a niobium-shielded tower of 22 mm inside diameter. The velocity of propagation of the interface in the column could be measured by magnetic means, as the magnetic susceptibility of the B phase is less than that of the A phase. The column had three sections of diameters 3.2, 1.6, and 0.8 mm to try to investigate the dependence of the velocity on macroscopic dimensions. The primary coil of the magnetometer consisted of two layers of closely wound 80-μm-diam Nb-Ti wire. The secondary coils consisted of three small astatically wound pairs made of the same wire and connected in series to the signal coil of a SQUID, one pair per section of the column. Further details of the apparatus can be found in ref. 10.

At the bottom of the column was another superconducting coil with a central field of 0.1? T/A. This coil provided a "valve" field which allowed precise control of the nucleation process in the column. The equilibrium transition temperature $T_{AB}$ is strongly suppressed by a magnetic field, falling to zero temperature at about 0.6 T. Thus, the introduction of the valve magnetic field between that part of the cell including the thermometer, in close thermal contact with the sinter and that part comprising the magnetometer separated the cell into two regions: that below the valve field, including the sinter

*Now at Biomagnetic Technologies, Inc., San Diego, CA 92121.

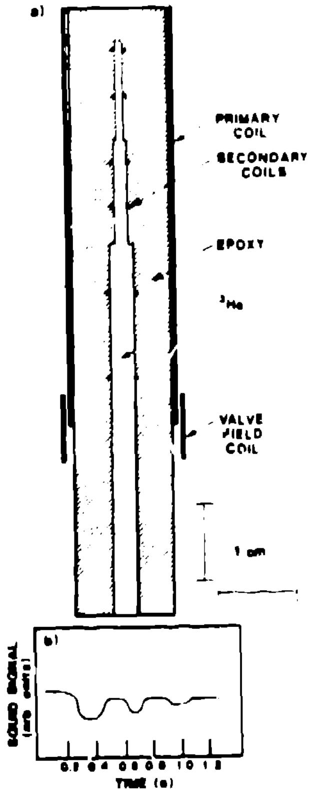


Fig. 1a. The A-B interfacial velocity cell.
1b. A typical signal generated in the six secondary coils as the A-B interface propagates through the cell from bottom to top.

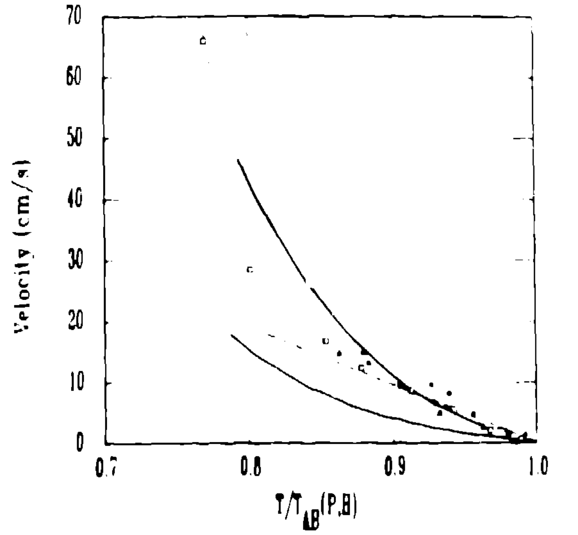


Fig. 2. Measured A-B phase-front velocity: squares, 33.6 bars, 10 mT; triangles, 29.7 bars, 10 mT; crosses, 24.5 bars, 20 mT; and lozenges, 29.7 bars, 40 mT. The measurements shown were obtained for the bottom (large diameter) section of the column, and, we believe, have $\hat{\ell}$ in the plane of the interface because of the applied magnetic field. The upper and lower solid lines are the values calculated by Yip and Leggett for $\hat{\ell}$ respectively normal and parallel to the plane of the phase boundary. The dashed line shows qualitatively the behavior predicted by Salomaa.

and the thermometer, and that above the valve field, i.e., the interior of the epoxy column. As a consequence, with the valve field set high enough that penetration of the B phase from either direction was impossible, nucleation occurred independently above and below the valve field. Since we found that nucleation always occurred first in the region below the valve field, it was straighforward [10] to let the B phase "pop" through the valve at the well defined temperature determined simply by the equilibrium A-B transition temperature in the high-field region of the valve. The phase boundary then propagated up the rest of the column in a hypercooled state. A typical magnetic signal as a function of time is shown in Fig. 1b, where the signals from the passage of the interface through each of the six secondary coils can clearly be seen. The velocity was calculated by measuring the time between the half-height points of the magnetization change indicated by succeeding coils and dividing by the distances between the centers of the coils.

We measured $v_{AB}$ for $T/T_{AB}$ between 0.99 and 0.77. The data for the lowest, largest-diameter section of the column are plotted versus $T/T_{AB}$ in Fig. 2 for three different pressures. The 33.6 and 29.7-bar data were taken in a 10-mT field while the 24.5-bar data were taken in a 20-mT field. Also plotted are data for 29.7 bars and 40 mT. All of the data fall on a common curve within experimental uncertainties. Velocities for the upper two sections of the column, not shown, were consistently slower than for the bottom section. But because of the design of the cell and the large temperature dependence of $v_{AB}$, we cannot conclude that $v_{AB}$ depends on tube diameter. A rough calculation shows that a heat leak as small as 5 pW down the column would also account for the velocity differences observed.

As discussed above, all of these measurements fall into the hypercooled regime, and so the classical thermal processes of diffusion of the latent heat away from the interface cannot determine the propagation velocity. Yip and Leggett [11] have proposed that under the conditions of these measurements the velocity is limited by transmission and Andreev reflection of quasiparticles, caused by the change in the order parameter across the interface. Their calculations of limiting velocities are possible because the quasiparticle mean free path is much larger than the effective width of the interface (which is of the order of the coherence length), so the calculations depend only on bulk A and B properties, not on the details of the spatial dependence of the wavefunction within the interface. Their calculations, shown in part in Fig. 2, are in reasonable agreement with our data and in addition predict several phenomena which have not yet been investigated experimentally: a strong dependence of $v_{AB}$ on the orientation of $\hat{\ell}$

in the A-phase; the possibility of underdamped interfacial waves at very low temperatures, where the interfacial inertial mass, of the order of $10^{-12}$g/cm$^2$, should dominate the dissipative Andreev reflection processes; a strong pressure-dependence of $v_{AB}$ near the polycritical point; and dominance of pair breaking over Andreev reflection as the velocity-limiting mechanism at very low temperatures, where $v_{AB}$ becomes comparable to the Fermi velocity.

Very recently, Salomaa [12] has predicted additional interesting characteristics of the moving A-B interface. Using symmetry analysis and numerical computations, he calculates the spatial dependence of the order parameter within the interface in detail, and predicts a textural transition within the interface at $v_{AB} \simeq 6$ cm/s, which he associates with the rapid increases in $v_{AB}$ that we observed (c.f. Fig. 2) below $T/T_{AB} \simeq 0.8$. He also predicts that, at lower temperatures and higher velocities, a new dissipation mechanism should dominate Andreev scattering: the emission of stable phase-slip plane excitations from the moving boundary.

## 3. NUCLEATION MECHANISMS

One of the most remarkable aspects of the A → B transition is that it occurs at all. This phase transition is of first order, with an exceedingly small bulk free energy difference between the two phases. Because of this small free energy difference, the energy of formation of a critical sized bubble of $^3$He-B in $^3$He-A, according to classical nucleation theory [13] and first estimated by Kaul and Kleinert [3], is $E_{bubble} \simeq 10^8 k_BT$, and the theoretical probability of homogeneous thermal nucleation, which is proportional to $\exp(-E_{bubble}/k_BT)$, is very roughly a hundred orders of magnitude smaller than the observed nucleation rate. Thus, the obvious experimental fact that the B phase does nucleate from supercooled A phase is not understood at all. Various alternate nucleation mechanisms, ranging from pathological distortion of the order parameter near boundaries to some heretofore unimagined flaw in our understanding of the statistical mechanics of extremely improbable processes, have been suggested; but none of these mechanisms has seemed probable enough to find general acceptance as an explanation of the nucleation puzzle.

A very novel alternative nucleation mechanism was proposed recently by Leggett [14]. He suggested that the nucleation of the B phase from the metastable A phase is caused by the passage of a cosmic ray through the $^3$He sample. The cosmic ray produces δ electrons along its path, and each δ electron quickly deposits its energy as heat in a "fireball" in the helium, with a radius of a few hundred angstroms. Leggett realized that the fireball would not reach thermal equilibrium with the rest of the fluid through ordinary diffusion of heat, because the quasiparticle mean free path in $^3$He is one to two orders of magnitude larger than the radius of the fireball. Consequently, he predicted that, at some time after its formation, the fireball would have the "baked Alaska" property: it would have a hot (but cooling) spherical shell propagating outward at nearly the Fermi velocity, surrounding a sphere of liquid at essentially the ambient liquid temperature. The expanding hot shell could protect nascent B phase inside it until the critical bubble radius was exceeded, so that the B phase could then expand to fill the experimental cell.

We undertook to check Leggett's hypothesis, to see if the passage of cosmic rays through a supercooled $^3$He-A sample caused the nucleation of $^3$He-B. Basically, we sandwiched a small sample of $^3$He between two particle detectors that could detect cosmic rays, as shown in Fig. 3. The $^3$He nucleation sample was isolated from most of the $^3$He in the cell by a region of high magnetic field. Magnetometers on the helium sample could detect the A → B phase transition. Repeatedly, we cooled the $^3$He from above the superfluid transition temperature through the A → B transition (slowly enough to ensure that the sample temperature was uniform to about 20 μK), monitoring the magnetometer and the two particle detectors, looking for three-way coincidences indicating the passage of a cosmic ray through the sample coincident with the nucleation of $^3$He-B. After monitoring 537 A → B transitions at 30 bar in this way, we had observed a statistically insignificant number of coincidences, suggesting that cosmic rays were not responsible for nucleation of the B phase.

However, we cannot definitively rule out all cosmic-ray-related nucleation mechanisms. The logic of this conclusion goes as follows. Because of the geometry of the sample and particle detectors, the angular distribution of incident cosmic rays, etc., we can calculate that we detected 30% of the cosmic rays that hit the $^3$He sample. If homogeneous, bulk cosmic-ray-induced nucleations were responsible for all A → B transitions in our sample, we would have detected 30% of such nucleations in coincidence with the cosmic rays we could observe, an easily distinguishable signal. So we can rule out homogeneous cosmic-ray-induced nucleation as originally proposed by Leggett. However, our data

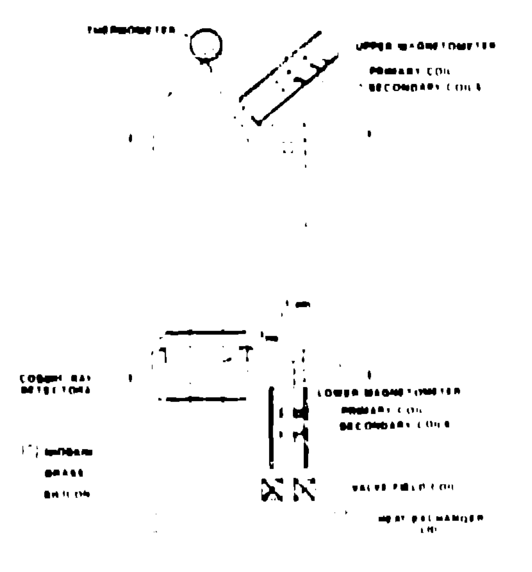

Fig. 3 Two cross sections through the cell used for cosmic ray induced nucleation

cannot eliminate the possibility that cosmic rays could be necessary and sufficient to add energy in the vicinity of a surface imperfection or textural singularity, causing nucleation at such sites only. Such sites could have been concentrated in the regions of our sample not covered by the particle detectors, so that we would never have detected the cosmic rays that triggered nucleations at those sites.

## 4. NUCLEATION LOCATIONS

This leads us to consider the locations of nucleation sites. Figure 4 illustrates how we determined nucleation locations in the simple geometry of the $v_{AB}$ apparatus. Locations were determined by measuring the relative timing of the magnetization-change signals from the six secondary coils in the column. During our ordinary $v_{AB}$ measurements, signals from the six coils occurred sequentially from bottom to top: 1, 2, 3, 4, 5, 6, as was shown in Fig. 1b. But with the valve field set high enough, nucleations occurred within the column. A typical resulting signal is shown in the inset to Fig. 4; there, the signals occurred in the order 2, 3, 1, 4, 5, 6, and it is easy to determine that the nucleation must have occurred somewhere in the plane labelled P = 30 bar in Fig. 4. Only three such nucleations were observed in that cell; their locations are marked in the figure.

The four secondary coils in the cosmic-ray cell also allowed us to obtain information on nucleation locations, and we collected a large amount of data, shown in Fig. 5, while we were looking for the cosmic-ray coincidences. We built the cosmic-ray cell before we learned that $v_{AB}$ is expected to depend strongly on A-phase texture, so there was no provision for controlling the texture throughout most of the sample. (In the $v_{AB}$ cell, the A-phase texture was well defined by the primary coil's magnetic field.) Since $v_{AB}$ may be anistropic with respect to texture by as much as a factor of three [11], it is impossible to translate the arrival time differences shown in Fig. 5 into nucleation locations unambiguously. The data are nevertheless intriguing. Firstly, the fact that there are two major, broad peaks in the curve of Fig. 5 shows that the nucleations were not simply occurring at the coldest part of the cell. Secondly, the existence of the two peaks in the data, but only one large, open region in the cell, suggests that the nucleation locations were not distributed throughout the cell in a spatially uniform way. Apparently there were two regions in the cell where nucleations most often occurred. This supports the suspicion that surfaces or textures are crucial parts of the nucleation mechanism.

## 5. NUCLEATION TEMPERATURES

We conclude with a brief discussion of the temperatures at which nucleations occurred. We show in Fig. 6 the nucleation temperatures we have observed in our two cells, at various pressures, and also nucleation temperatures observed in a rotating NMR apparatus in Helsinki [15]. In the figure caption we list the conditions for each of the points on the plot. It is striking that the nucleation temperatures varied so widely under different circumstances. Equally striking is the fact that for a given set of conditions, the nucleation temperatures were very reproducible.

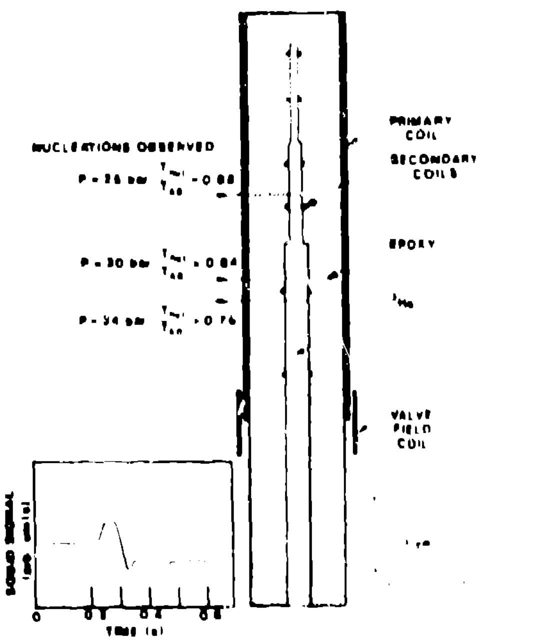


Fig. 4 Locations of B phase nucleations in the interfacial velocity cell. The inset at lower left shows the signal generated in the 6 secondary coils after the P = 30 bar nucleation.

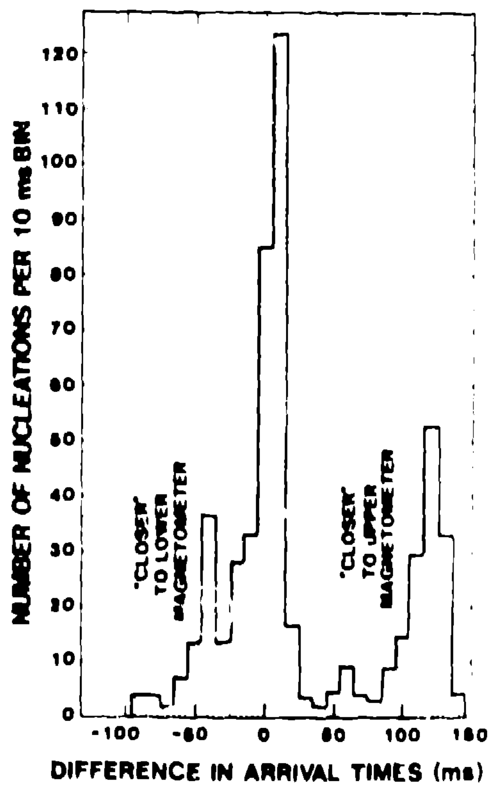


Fig. 5 A histogram of differences in arrival times of the A-B interface at the upper and lower magnetometers in the cosmic ray cell.

for example, the 537 nucleations observed in our cosmic-ray cell occurred at $T_n/T_{AB}$ = 0.919 with a standard deviation of only 1.3%. These data suggest that magnetic field strength exerts an important influence on nucleation temperature, with the nucleation temperature being suppressed by magnetic field far more strongly than the equilibrium transition temperature is suppressed. Systematic, accurate measurements of the magnetic field dependence of the nucleation temperature may be one key to the understanding of the nucleation process.

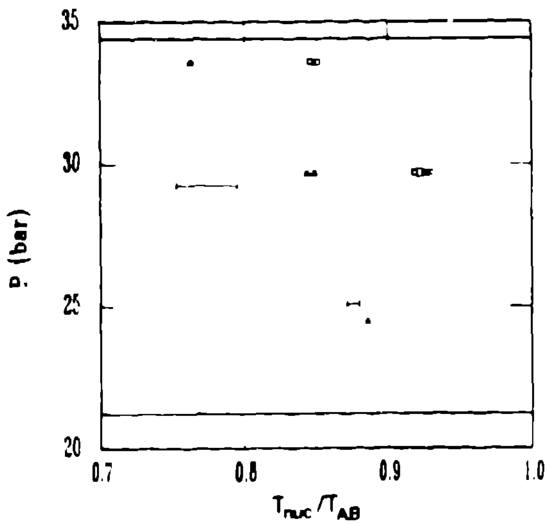


Fig. 6. B-phase nucleation temperatures under a variety of circumstances. Squares: interfacial velocity cell, "below" the valve field (sinter and thermometer), 0 gauss. Triangles: interfacial velocity cell, "above" the valve field (magnetometer column), 100 gauss (30 and 34 bar) and 200 gauss (25 bar). Circle: cosmic-ray cell, both "above" and "below" the valve field, 0 gauss. Horizontal lines: Helsinki rotating NMR apparatus, few hundred gauss.

ACKNOWLEDGEMENTS

We are most grateful to the late John Wheatley for inspiration and support. We would like to thank Doug Osheroff for suggesting the valve field, and Tony Leggett, Sungkit Yip, and Gordon Baym for many enlightening discussions about the A-B interface. Steve Boyd, who is continuing this work, collected much of the data with the cosmic-ray cell. This work is supported by the Division of Materials Science in DOE's Office of Basic Energy Sciences.

REFERENCES

1) D. D. Osheroff and M. C. Cross, Phys. Rev. Lett. 38, 905 (1977).
2) M. C. Cross, in Quantum Fluids and Solids, edited by S. B. Trickey, E. D. Adams, and J. W. Dufty (Plenum, New York, 1977).
3) R. Kaul and H. Kleinert, J. Low Temp. Phys. 38, 553 (1980).
4) N. Schopohl, Phys. Rev. Lett. 58, 1664 (1987).
5) S. Yip, Phys. Rev. B32, 2915 (1985).
6) M. M. Salomaa, Nature 326, 367 (1987).
7) J. H. Perepezko, in Proceedings of the Second International Conference on Rapid Solidification Processing, edited by R. Mehrabian, B. H. Kear, and M. Cohen (Claitor's Publishing Division, Baton Rouge, LA, 1980), p. 56.
8) F. Spaepen and D. Turnbull, in Laser Annealing of Semiconductors, edited by J. M. Poate and J. W. Mayer (Academic, New York, 1983), p. 15.
9) S. Yip, private communication.
10) D. S. Buchanan, G. W. Swift, and J. C. Wheatley, Phys. Rev. Lett. 57, 341 (1986).
11) S. Yip and A. J. Leggett, Phys. Rev. Lett. 57, 345 (1986).
12) M. M. Salomaa, preprint.
13) R. Becker and W. Doring, Ann. Phys. 24, 719 (1935).
14) A. J. Leggett, Phys. Rev. Lett. 53, 1096 (1984).
15) P. J. Hakonen, M. Krusius, M. M. Salomaa, and J. T. Simola, Phys. Rev. Lett. 54, 245 (1985).